Eur. Phys. J. B (2013) 86: 274
DOI: 10.1140/epjb/e2013-30964-y

THE EUROPEAN PHYSICAL JOURNAL B

Regular Article

Transmittance and reflectance measurements at terahertz frequencies on a superconducting $BaFe_{1.84}Co_{0.16}As_2$ ultrathin film: an analysis of the optical gaps in the Co-doped $BaFe_2As_2$ pnictide

Andrea Perucchi[1], Leonetta Baldassarre[1,a], Boby Joseph[2], Stefano Lupi[3], Sanghan Lee[4], Chang Beom Eom[4], Jianyi Jiang[5], Jeremy D. Weiss[5], Eric E. Hellstrom[5], and Paolo Dore[6,b]

[1] Sincrotrone Trieste, S.C.p.A., Area Science Park, 34012 Basovizza, Trieste, Italy
[2] Dipartimento di Fisica, Università di Roma Sapienza, P.le Aldo Moro 2, 00185 Roma, Italy
[3] CNR-IOM and Dipartimento di Fisica, Università di Roma Sapienza, P.le Aldo Moro 2, 00185 Roma, Italy
[4] Department of Materials Science and Engineering, University of Wisconsin-Madison, Madison, WI 53706, USA
[5] Applied Superconductivity Center, National High Magnetic Field Laboratory, Florida State University, 2031 East Paul Dirac Drive, Tallahassee, FL 32310, USA
[6] CNR-SPIN and Dipartimento di Fisica, Università di Roma Sapienza, P.le Aldo Moro 2, 00185 Roma, Italy

Received 22 October 2012 / Received in final form 22 March 2013
Published online 17 June 2013 –

Abstract. Here we report an optical investigation in the terahertz region of a 40 nm ultrathin $BaFe_{1.84}Co_{0.16}As_2$ superconducting film with superconducting transition temperature $T_c = 17.5$ K. A detailed analysis of the combined reflectance and transmittance measurements showed that the optical properties of the superconducting system can be described in terms of a two-band, two-gap model. The zero temperature value of the large gap Δ_B, which seems to follow a BCS-like behavior, results to be $\Delta_B(0) = 17$ cm^{-1}. For the small gap, for which $\Delta_A(0) = 8$ cm^{-1}, the temperature dependence cannot be clearly established. These gap values and those reported in the literature for the $BaFe_{2-x}Co_xAs_2$ system by using infrared spectroscopy, when put together as a function of T_c, show a tendency to cluster along two main curves, providing a unified perspective of the measured optical gaps. Below a temperature around 20 K, the gap-sizes as a function of T_c seem to have a BCS-like linear behavior, but with different slopes. Above this temperature, both gaps show different supra-linear behaviors.

1 Introduction

After more than four years since the discovery of high-temperature superconductivity in the iron pnictide LaFeAsO [1], the interest in the Fe-based superconductors (FeBS) is far from declining. Few months after this very first announcement, superconductivity was reported up to 55 K in F-doped SmFeAsO [2]. Despite several progresses in discovering similar superconducting families, the 55 K value still remains the highest T_c observed so far in a FeBS. Although it will be possible that such a limit may never be beaten by these compounds, the true opportunity offered by the FeBS at this moment is in providing new clues towards the understanding of the high-temperature superconductivity phenomenon [3]. As pointed out by many authors, FeBS present important similarities with copper-oxides, but, at variance with cuprates, the complex electronic structure of FeBS is associated with all the five iron 3*d* orbitals, thus giving origin to a well-recognized multi-band character. The first question which then naturally arises is whether multiple superconducting gaps originate from multiple bands. Such a question was already addressed theoretically by Suhl, Matthias and Walker back in 1959 [4], shortly after the formulation of the BCS theory for superconductivity. It was found that the presence of multiple bands crossing the Fermi level does not necessarily imply multi-gap superconductivity. In fact, contrary to single-band superconductors, the presence of impurities plays a very central role, since even non-magnetic impurities can act as pair-breakers. This gives rise to gaps merging and to a depression of superconductivity. Such a detrimental role of impurities to superconductivity is however not observed if the impurities scatter quasi-particles within the same electronic band. This is indeed the case of MgB_2, where the interband scattering is rather weak [5,6]. In FeBS, an accurate determination of symmetry and sizes

[a] *Present address*: Center for Life NanoScience@LaSapienza, Istituto Italiano di Tecnologia, Viale Regina Elena 295, Roma, Italy.
[b] e-mail: paolo.dore@roma1.infn.it

of the superconducting gap(s) is necessary since five bands must be considered in describing the electronic properties of the system [7–11], although simplified models in which only two bands are considered, can capture the essential low-energy physics of the unconventional superconductivity in these systems [12–15].

From the experimental viewpoint, evidences on multiple gaps in FeBS are not as conclusive as in the case of MgB_2 [6]. Indeed, the observed gaps vary in number and symmetry, and are sometimes accompanied by the presence of ungapped states, either attributed to nodes or to the presence of pair-breakers [7–11]. This wide variety of results is usually explained by differences in sample quality, disorder, variable doping level, and by the different sensitivity of the various experimental techniques with respect to one gap or another. Therefore, further efforts are necessary to clarify the reason of apparently contradictory results.

Among FeBS, compounds of the so-called 122 family [16,17] (e.g. $BaFe_2As_2$), in which superconductivity can be achieved both by electron or hole doping, can be of particular importance in studying superconducting gaps. In particular, the $BaFe_{2-x}Co_xAs_2$ system has been selected for several studies to obtain reliable results not affected by the sample quality issue, thanks to the possibility to grow high-quality single crystals and films, with controlled Co doping and highly reproducible transport and superconducting properties. In this system, the electronic and superconducting properties have been widely investigated through a variety of different experimental techniques, such as ARPES (angle resolved photoemission spectroscopy) [18–23], STS (scanning tunneling spectroscopy) [24], calorimetry [25], PCAR (Point-Contact Andreev-Reflection) [26]. Also infrared investigation has been widely employed since it can be of particular interest in studying low-energy electrodynamics of strongly correlated electron systems [27,28], and indeed it provided several important inputs on the electronic and superconducting properties of the $BaFe_{2-x}Co_xAs_2$ system [29–49]. A number of studies have been particularly addressed to the determination of the superconducting gaps [36–49]. Indeed, as evidenced since the pioneering works from Tinkham and collaborators [50–52], infrared measurements in the terahertz (THz) region can be a powerful tool to detect the superconducting gap(s). However, for the $BaFe_{2-x}Co_xAs_2$ system, the reported number of gaps range from one to three, with very different sizes [36–49]. Understanding the reasons underlying these discrepancies among optical investigations is highly desirable, if one really wants to take advantage of the unique potential of the optical techniques in terms of the energy resolution and the bulk sensitivity.

In the present paper we report combined transmittance and reflectance measurements at THz frequencies on a $BaFe_{1.84}Co_{0.16}As_2$ ultrathin (40 nm) film deposited on a $LaAlO_3$ substrate, with superconducting transition temperature $T_c = 17.5$ K. Obtained results show evidence for a two-band, two-gap structure in an ultra-thin film, in which T_c is reduced with respect to the case of optimal single crystals. The superconducting gaps we obtained and those reported in the literature by infrared spectroscopy in $BaFe_{2-x}Co_xAs_2$ system, when put together as a function of T_c, show a tendency to cluster along two main curves, thus allowing to describe the seemingly contradictory reports [36–49] into a unified perspective.

2 Experimental

High quality Co-doped $BaFe_2As_2$ films are grown by pulsed laser deposition on $SrTiO_3$ (STO) [53]. Even in the highest quality single-crystalline films with thickness of the order of 400 nm, the T_c value is slightly lower than that reported for single crystals (∼25 K [54]). The reduced T_c value in an optimally doped compound is attributed to the presence of vortex-pinning columnar defects [53]. For further informations on the film growth and on their epitaxial quality see reference [53].

For the present optical investigation, we employed a $BaFe_{1.84}Co_{0.16}As_2$ (BFCA) film (thickness 40 nm) grown on a $LaAlO_3$ (LAO) substrate (0.5 mm thick) with a 20 nm STO intermediate layer to allow epitaxial growth. Since very thin films can be unstable upon air exposure, the film was covered by a 10 nm thick protective Pt cap-layer. Note that the back surface of the LAO substrate was also optically polished and thoroughly cleaned before the optical measurements. Such a thin film does not have optimal transport and superconducting properties. Indeed, resistivity measurements (inset in Fig. 1) on a film equivalent to the one we employed for optical measurements (same heterostructure LAO/STO/BCFA) provided a critical temperature $T_c = 17.5$ K (where T_c is measured at half width of the resistivity curve, with $\Delta T_c = 1.4$ K). Nonetheless, LAO is transparent up to about 140 cm^{-1} (about 4 THz) at low temperatures [55], and thus a 40 nm thin film deposited on LAO provides the opportunity to combine transmittance and reflectance measurements on the same sample, thus allowing, at least in principle, a strongly constrained analysis of the optical data [56].

Measurements were performed using synchrotron radiation as an intense THz source, at the SISSI beamline [57] of the Elettra synchrotron operating at 2.4 GeV in stable top-up mode, and a Bruker IFS66v spectrometer equipped with Si-bolometers. The film was mounted in a liquid He flow cryostat Helitran LT-3 coupled to the interferometer. By mounting the sample over one of the two holes in the sample holder, we could measure its absolute transmittance spectrum, $\mathcal{T}(T)$, as a function of the temperature. The absolute intensity of the $\mathcal{T}(T)$ spectra are slightly uncertain, in particular at low frequency, because of possible misalignments due to the necessity of reference measurements. In order to avoid this problem, we mostly performed relative measurements, by cycling the temperature without moving the sample. Besides the transmittance ratios, $\mathcal{T}(T)/\mathcal{T}_N$, we also measured the reflectance ratios, $\mathcal{R}(T)/\mathcal{R}_N$, with $\mathcal{T}_N$ and $\mathcal{R}_N$ being the $T = 20$ K normal state transmittance and reflectance. The advantage of this technique, successfully adopted in the past [50–52], is that all temperature-driven distortions of the optical set-up are

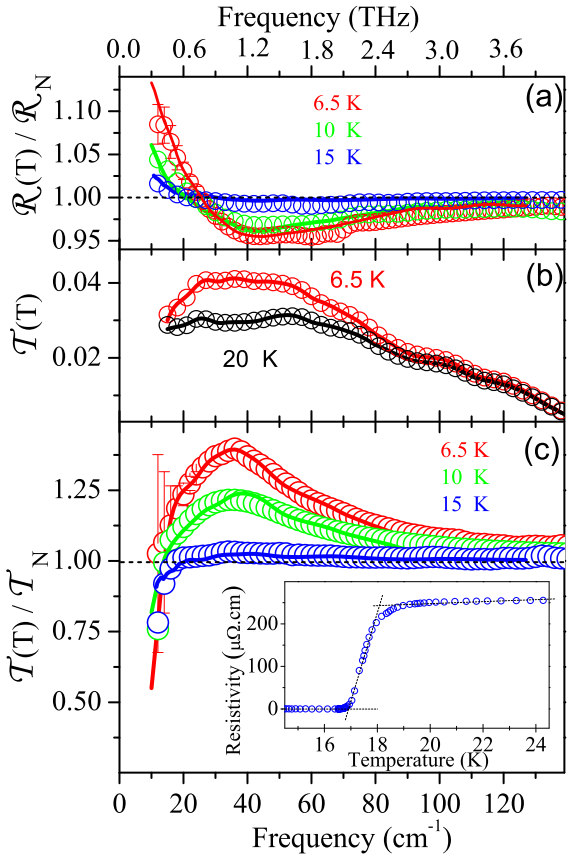

Fig. 1. (a) Reflectance ratios $\mathcal{R}(T)/\mathcal{R}_N$. Empty circles are data points, full lines are the fits performed with the 15-oscillators-model (see text). (b) Absolute transmittance $\mathcal{T}(T)$ at 6.5 and 20 K. (c) Same as in (a) for the transmittance ratios $\mathcal{T}(T)/\mathcal{T}_N$. In (a) and (c), typical error bars affecting low frequency data are only reported for the 6.5 K data for sake of clarity. Inset in (c) shows the results of resistivity measurement on a film equivalent to the one employed in the optical measurement (i.e. same LAO/STO/BCFA heterostructure but no Pt cap layer). T_c measured at half width is 17.5 K, with $\Delta T_c = 1.4$ K.

already freezed around 20 K, thus making unnecessary the reference measurement at every temperature.

Figures 1a and 1c, respectively report the reflectance ratios $\mathcal{R}(T)/\mathcal{R}_N$ and the transmittance ratios $\mathcal{T}(T)/\mathcal{T}_N$ measured at 6.5, 10, and 15 K. We remark that the use of a high-flux synchrotron source and the large size of the thin film surface, besides allowing transmittance measurements, enables addressing the low frequency reflectivity with superior signal to noise ratio with respect to measurements on single crystals. The absolute transmittance, as reported in Figure 1b at two selected temperatures (20 and 6.5 K), is limited up to a maximum frequency of 140 cm^{-1} by the absorption from the LAO substrate [55]. As predicted by the standard BCS Mattis-Bardeen relations [58,59], at least for a one-band isotropic s-wave superconductor at $T \ll T_c$, a maximum at the optical gap 2Δ is expected either in $\mathcal{R}(T)/\mathcal{R}_N$ for a bulk sample, or in $\mathcal{T}(T)/\mathcal{T}_N$ for a thin film. It is important to recall that, in the case of a thin film on a transparent substrate, $\mathcal{R}(T)/\mathcal{R}_N$ at $T \ll T_c$ does not necessarily exhibit a maximum, but increases with decreasing frequency [56]. As evident from Figure 1, $\mathcal{T}(T)/\mathcal{T}_N$ and $\mathcal{R}(T)/\mathcal{R}_N$ data at 6.5 K, as well as their progressive flattening with increasing temperature, are well consistent with these predictions. We remark that, as already noticed in the past [60], the effect of the superconducting transition on the transmittance ratio is larger than on the reflectance ratio. Therefore, the $\mathcal{T}(T)/\mathcal{T}_N$ measurement can have a key role in a precise determination of the superconducting gap(s).

3 Analysis

The analysis of optical data like those of Figure 1 is aimed at determining the complex conductivity $\tilde{\sigma}(\omega) = \sigma_1(\omega) + i\sigma_2(\omega)$ which is usually introduced in discussing the low energy electrodynamics of the system. In the case of a bilayer system (film deposited on substrate), a first possible procedure (procedure *P1*) consists of different steps: (i) modeling the $\tilde{\sigma}(\omega)$ in terms of a given set of parameters; (ii) deriving a model (complex) refractive index $\tilde{n}(\omega) = n(\omega) + ik(\omega)$ by using standard equations [61]; and (iii) evaluating model reflectance and/or transmittance spectra by using standard relations [59,60,62] which require the knowledge of $\tilde{n}(\omega)$ and thickness of film and substrate. In the final step (iv), the model spectrum is fitted to the experimental one to obtain the relevant parameters which determine the film conductivity $\tilde{\sigma}(\omega)$.

In step (i), the Drude model is usually employed to describe the $\tilde{\sigma}(\omega)$ in the normal state: a contribution centered at zero frequency (Drude contribution, with parameters plasma frequency Ω and scattering rate γ) describes free-charges in a conduction band. Below T_c, the Drude term can be conveniently substituted by the Zimmermann term [63], which generalizes the standard BCS Mattis-Bardeen model [58,59] to arbitrary T and γ values, with the inclusion of two additional parameters, the superconducting gap Δ and the ratio T/T_c. For convenience, this model will be hereafter referred as the DZ (Drude-Zimmermann) model. When two (or more) bands contribute to the film conductivity, the parallel conductivity model can be employed [60,64], in which the total conductivity is simply given by the sum of single-band contributions. In the present case, we use a two-band model [12–15], which has been widely employed in describing the optical (see for example Refs. [36,37,39,41]) and several other properties (see for example Refs. [25,26]) of the $BaFe_{2-x}Co_xAs_2$ system.

In the past, we have successfully employed procedure *P1* in the analysis of the optical response in the THz region of a thick $BaFe_{1.84}Co_{0.16}As_2$ film [42], as well as that of two-band systems such as MgB_2 [64,65], CaAlSi [66] and V_3Si [60]. However, in the present case, it is important to remind that the optical response of the sample, while being dominated by the BFCA film (40 nm) and by the LAO substrate (0.5 mm), is also affected by the presence of the Pt cap-layer (10 nm) and of the STO buffer layer

(20 nm). Therefore, it is necessary to consider a four-layer system (Pt-film-STO-LAO) and to to evaluate its optical response [59] from the $\tilde{n}(\omega)$ and thickness of each layer. For STO and LAO crystals, detailed data on the temperature dependence of $\tilde{n}(\omega)$ are available [55,67,68]. In the case of a thick BFCA film on LAO, it was found that a thin intermediate STO layer does not appreciably affect the model spectra of the three-layer system [40,42]. In the present case of the four-layer system, we verified that, even by employing the $\tilde{n}(\omega)$ values derived in the case of a thin STO film [69], the effect of the STO layer can be anyway neglected. On the contrary, the effect of the Pt cap layer cannot be neglected. Indeed, independent measurements performed on an ad hoc reference sample in which a Pt layer was deposited on LAO showed that the Pt layer has an important screening effect, which in the THz region be accounted for by a broad featureless Drude contribution.

To analyze the present data, procedure *P1* has thus been modified in step (iii) in order to consider a three-layer system (Pt-film-LAO) and to evaluate the model spectra to be fitted to the measured ones in step (iv). However, the direct simultaneous fitting of $\mathcal{R}_S/\mathcal{R}_N$ (with $\mathcal{R}_S = \mathcal{R}$ (6.5 K)) and $\mathcal{T}_S/\mathcal{T}_N$ (with $\mathcal{T}_S = \mathcal{T}$ (6.5 K)) turned out to be far from trivial, if the previous knowledge of the normal state parameters is missing. To this end, a model independent determination of the optical conductivity would be highly desirable in order to clearly determine the low energy excitations necessary to our analysis.

The availability of both reflectance and transmittance ratios does in principle provide the possibility to extract $\tilde{\sigma}(\omega)$ without relying on theoretical models, through an inversion procedure, recently adopted by Xi et al. [56] in the case of a film-substrate system. In our case, the presence of the Pt cap layer on top of the film makes the inversion procedure exceedingly complicated and does not provide reliable results.

We have then employed a different procedure (procedure *P2*), which is equivalent to *P1*, except for step (i). In step (i), instead of using the DZ model to describe $\tilde{\sigma}(\omega)$, we have employed a large number of Lorentz oscillators (15, one in every 10 cm^{-1}), in the same spirit of the so-called Kramers-Kronig constrained analysis pioneered by Kuzmenko in 2005 [70]. For convenience, this model will be hereafter referred as the "15-oscillators-model". We remark that, within such an approach, each Lorentzian oscillator is not associated to a given physical excitation, but rather represents the elementary building block for a Kramers-Kronig consistent description of the optical functions. The large number of oscillators provides the necessary flexibility to reproduce the experimental data points with the highest accuracy, thus making the extraction of the film $\tilde{\sigma}(\omega)$ substantially model-independent. Steps (ii) and (iii) are the same as in procedure *P1*, in step (iv) we simultaneously fitted model spectra to the experimental $\mathcal{T}(T)/\mathcal{T}_N$ and $\mathcal{R}(T)/\mathcal{R}_N$ at any given temperature. Also the absolute transmittance $\mathcal{T}(T)$ data have been fitted with the same procedure. As evident from Figure 1, this procedure provides good fits (continuous lines) of the experimental results, for all temperatures.

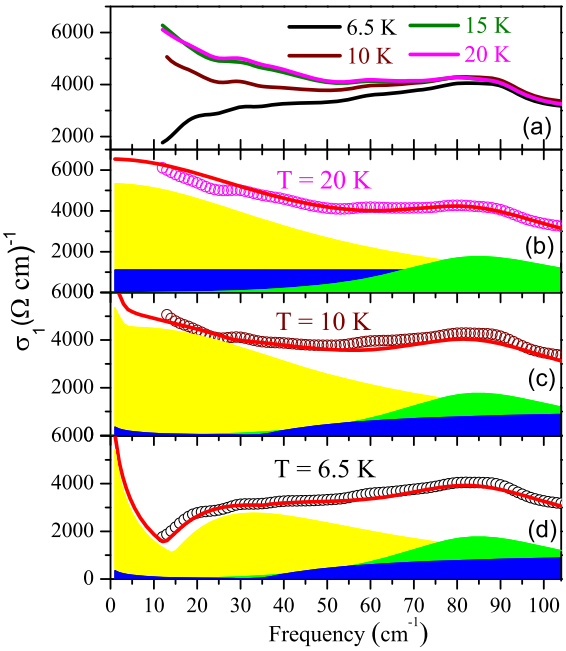

Fig. 2. (a) Optical conductivity of the BCFA thin film with $T_c = 17.5$ K, as extracted from the 15-oscillators-model, at 20, 15, 10, and 6.5 K. (b) Lorentz-Drude fit (red solid line) of the normal state conductivity (open circles) with 2 Drude components (yellow and blue) and one low energy Lorentzian oscillator (green). (c) and (d) same as in (b) at 10 and 6.5 K with the two Drude terms modified by the opening of a superconducting gaps described by the Zimmermann term [63].

4 Discussion

In discussing the information provided by the complex conductivity $\tilde{\sigma}(\omega)$, its real part $\sigma_1(\omega)$ (optical conductivity) is usually considered. The temperature dependence of the $\sigma_1(\omega)$ up to 110 cm^{-1}, obtained from the 15-oscillators-model is reported in Figure 2. The 20 K optical conductivity monotonously decreases with increasing frequency except for a bump located at about 85 cm^{-1}. Such feature has already been observed [41,46], and can be interpreted as an intrinsic excitation [71], due to the onset of interband transitions caused by the presence of several bands crossing the Fermi level.

With decreasing temperature, the optical conductivity is depleted at low frequencies as a consequence of the opening of superconducting gap(s). At high frequencies, all conductivity curves merge above 90 cm^{-1}. It is easily recognized that even at the lowest temperature (6.5 K, i.e. $\sim 0.4T_c$), the gapping is not complete. The presence of finite conductivity at low frequencies, well into the superconducting state, has been interpreted in terms of pair-breaking [40], nodal symmetries [37,45], or to the presence of a band in which there is no gapping [46] or the gap opens at such a low energy that its presence is difficult to be detected. However, it is to be noted that, in the present case, also the Pt cap-layer might give a finite contribution at frequencies below the superconducting gap.

On the above basis, we described the normal state $\sigma_1(\omega)$ by two Drude terms and by one Lorentzian oscillator

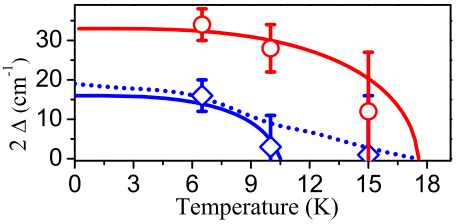

Fig. 3. Gap values obtained from the data analysis at different temperatures. Here the red line indicates the BCS-like behavior of the gap Δ_B, the blue-line a BCS-like behavior of the gap Δ_A with a reduced T_c, and the dotted-blue-line is a guide to the eye indicating a possible non-BCS temperature dependence of Δ_A (see text).

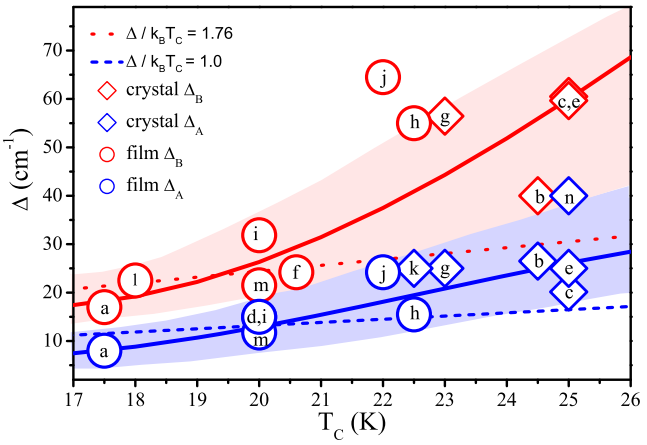

Fig. 4. Gap values reported from optical data on $BaFe_{2-x}Co_xAs_2$ compounds [36–49]. Red (blue) symbols refer to large (small) gaps. Diamonds (circles) markers are data related to crystals (films). Label "a" represents the gap values obtained in the present study. The labels "b" to "n" are respectively from references [36] to [49]. Thick solid lines (red and blue) are guides to the eye. The dotted red line corresponds to the expectation from BCS weak coupling $\Delta/k_BT_c = 1.76$, the dashed blue line represents $\Delta/k_BT_c = 1.0$.

mimicking the low-energy interband transition, as shown in Figure 2b. Because of the restricted spectral range of our data, it is possible to obtain a reasonable determination of the narrow Drude term (A), with plasma frequency $\Omega_A \approx 4000$ cm^{-1}, scattering rate $\gamma_A \approx 50$ cm^{-1}, and corresponding dc conductivity $\sigma_{0A} \approx 5300\,\Omega^{-1}$ cm^{-1}. On the other hand the broad Drude term (B), which basically acts as a background in the explored frequency range, cannot be reliably estimated (very approximate values for its parameters are $\Omega_B \sim 10\,000$ cm^{-1}, $\gamma_B \sim 1500$ cm^{-1}, $\sigma_{0B} \sim 1100\ \Omega^{-1}$ cm^{-1}). We recall that the presence of two Drude terms with very different widths has been adopted by many authors to describe the optical properties of $BaFe_{2-x}Co_xAs_2$ systems (see for example Refs. [35,49,72]).

In the superconducting state (at 6.5, 10 and 15 K), the same components (two Drude and one Lorentzian terms) are used to fit the $\sigma_1(\omega)$, with each of the two Drude terms modified by the opening of a superconducting gap described by the Zimmermann term. This fitting procedure, with the gap values Δ_A and Δ_B being the two unique free parameters, provides good descriptions of the $\sigma_1(\omega)$, as shown in Figure 2c for $T = 10$ K and Figure 2d for $T = 6.5$ K.

The gap values resulting from the above procedure are reported in Figure 3 as a function of temperature. We remark that the small gap values are affected by a rather large uncertainity since they are close to the lower experimental detection limit. The temperature dependence of the large gap Δ_B seems to follow a BCS-like behavior, in accordance with the results of ARPES [18], STS [24] and PCAR [26] studies. On the contrary, the small gap Δ_A appears to be strongly depressed already at 10 K, which may suggest that the temperature dependence is not compatible with a BCS behaviour, as suggested by the dotted line in Figure 3. Although no definitive assessment can be made, the present data may both suggest that a weak interband scattering becomes effective with reduced T_c [43,44], or that the small gap closes at about $0.6T_c$ in the $BaFe_{2-x}Co_xAs_2$ system. In spite of these uncertainties, on the basis of the data reported in Figure 3, we can safely quote that the zero-temperature gap values are $\Delta_A(0) = 8 \pm 3$ cm^{-1} and $\Delta_B(0) = 17 \pm 1$ cm^{-1}.

But how does this result compare with previous reports on the $BaFe_{2-x}Co_xAs_2$ system? The values of the small (Δ_A) and large (Δ_B) gaps as a function of T_c, as determined (in the zero-temperature limit) from all the optical measurements we were aware of [36–49] are presented in Figure 4. From this plot, it can be readily observed that the gap values show a tendency to cluster along two main curves (thick solid lines in Fig. 4). The comparison with the weak-coupling BCS prediction ($\Delta(0)/k_BT_c = 1.76$, dotted line in Fig. 4) shows that the T_c dependence of the large gap Δ_B may be compatible with a BCS linear behavior up to about 20 K, while a supra-linear behavior at higher T_c values. As to the small gap Δ_A, a linear behaviour might be hypothesized again up to about 20 K, with a slope $\Delta_A(0)/k_BT_c = 1.0$ (dashed line in Fig. 4), much lower than the weak-coupling BCS value. Similar to the case of Δ_B, the smaller gap also shows a supra-linear behavior above 20 K.

In discussing the results reported in Figure 4, it is worth to recall that Hardy et al. [25], through an extensive calorimetric study of $BaFe_{2-x}Co_xAs_2$ single-crystals with different Co content (i.e., with different T_c), have observed a linear T_c dependence of the large gap Δ_B, with the onset of a slight supra-linear behavior above 20 K. As to the small gap Δ_A, specific heat measurements [25] showed a linear behaviour with $2\Delta/k_BT_c = 0.95$, in reasonable agreement with the results reported shown in Figure 4 up to 20 K, but without the onset of any supra-linear behaviour. This difference between the results of optical and calorimetric techniques cannot at the moment be explained and is rather surprising, especially in the light of the bulk sensitivity of both techniques. Still, both optical data and specific heat demonstrate that in the case of the $BaFe_{2-x}Co_xAs_2$ system the deviations from a BCS linear behavior are not large for compounds with low T_c ($\lesssim$20 K), and an overall weak coupling scenario thus applies.

5 Conclusion

We have addressed in this work the superconducting gap properties of an ultrathin (40 nm) $BaFe_{1.84}Co_{0.16}As_2$ film. The reduced film thickness and the $LaAlO_3$ substrate allowed combined transmittance and reflectance measurements. In particular, we measured the transmittance and reflectance ratio between the superconducting and normal state, which is a powerful tool to determine the superconducting gap(s). A detailed data analysis shows that, even in the case of a depleted T_c value, the system displays characteristic features of two-band, two-gap superconductivity. The zero temperature value of the large gap Δ_B, which seems to follow a BCS-like behavior, results to be $\Delta_B(0) = 17$ cm^{-1}. For the small gap, for which the temperature dependence cannot be clearly established, we quote $\Delta_A(0) = 8$ cm^{-1}.

The gap values we obtain and those reported in the literature for the $BaFe_{2-x}Co_xAs_2$ by using infrared spectroscopy [36–49], when put together as a function of the superconducting transition temperature T_c, show a tendency to cluster along two main curves, providing a unified perspective of the measured optical gaps. The large gap values show a weak-coupling BCS temperature dependence (with $\Delta_B/k_BT_C \sim 1.76$), with the onset of a slight supra-linear behavior above 20 K, in agreement with the results of an extensive calorimetric study [25]. Also the small gap Δ_A seems to show a linear behaviour with $\Delta_A/k_BT_C \sim 1.0$, with the onset of a slight supra-linear behaviour above 20 K, at variance with the calorimetric study where a linear behaviour is always observed.

In conclusion, both optical and specific heat data demonstrate that in the case of the $BaFe_{2-x}Co_xAs_2$ system, the deviations from a BCS linear behavior are not remarkable, in particular for compounds with low T_c ($\lesssim$20 K), and an overall weak coupling scenario seems to be valid. To observe more important deviations from the BCS trend within Fe-based materials, which may be indicative of a weak to strong coupling crossover, one should consider superconductors with even higher T_c, as in the $Ba_{1-x}K_xFe_2As_2$ family [25] or within oxypnictides [3].

Work at the Sapienza University of Rome was partially supported by the Cariplo Foundation (Project No. 2009-2540). The authors thank L. Boeri for helpful discussions. Work at the University of Wisconsin was supported by funding from the DOE Office of Basic Energy Sciences under award number DE-FG02-06ER46327. The works at the NHMFL was supported under NSF Cooperative Agreement DMR-0654118 and DMR-1006584, by the State of Florida.

References

1. Y. Kamihara, T. Watanabe, M. Hirano, H. Hosono, J. Am. Chem. Soc. **130**, 3296 (2008)
2. Z.-A. Ren, G.-C. Che, X.-L. Dong, J. Yang, W. Lu, W. Yi, X.-L. Shen, Z.-C. Li, L.-L. Sun, F. Zhou, Z.-X. Zhao, Europhys. Lett. **83**, 17002 (2008)
3. D.S. Isonov, J.T. Park, A. Charnuka, Y. Li, A.V. Boris, B. Keimer, V. Hinkov, Phys. Rev. B **83**, 214520 (2011)
4. H. Suhl, B.T. Matthias, L.R. Walker, Phys. Rev. Lett. **3**, 552 (1959)
5. I.I. Mazin, O.K. Andersen, O. Jepsen, O.V. Dolgov, J. Kortus, A.A. Golubov, A.B. Kuzmenko, D. van der Marel, Phys. Rev. Lett. **89**, 107002 (2002)
6. X.X. Xi, Rep. Prog. Phys. **71**, 116501 (2008)
7. P. Richard, T. Sato, K. Nakayama, T. Takahashi, H. Ding, Rep. Prog. Phys. **74**, 124512 (2011)
8. D. Daghero, M. Tortello, G.A. Ummarino, R.S. Gonnelli, Rep. Prog. Phys. **74**, 124509 (2011)
9. Fa Wang, Dung-Hai Lee, Science **332**, 200 (2011)
10. O.K. Andersen, L. Boeri, Ann. Phys. **523**, 8 (2011)
11. J.P. Hirschfeld, M.M. Korshunov, I.I. Mazin, Rep. Prog. Phys. **74**, 124508 (2011)
12. S. Raghu, X.-L. Qi, C.X. Liu, D.J. Scalapino, S.C. Zhang, Phys. Rev. B **77**, 220503(R) (2008)
13. Q. Han, Y. Chen, Z.D. Wang, Europhys. Lett. **82**, 37007 (2008)
14. A. Nicholson, W. Ge, X. Zhang, J. Riera, M. Daghofer, A.M. Oles, G.B. Martins, A. Moreo, E. Dagotto, Phys. Rev. Lett. **106**, 217002 (2011)
15. A. Charnukha, V. Dolgov, A. A. Golubov, Y. Matiks, D.L. Sun, C.T. Lin, B. Keimer, A.V. Boris, Phys. Rev. B **84**, 174511 (2011)
16. P.C. Canfield, S.L. Budko, Annu. Rev. Condens. Matter Phys. **1**, 27 (2010)
17. H.H. Wen, S. Li, Annu. Rev. Condens. Matter Phys. **2**, 121 (2011)
18. K. Terashima, Y. Sekiba, J.H. Bowen, K. Nakayama, T. Kawahara, T. Sato, P. Richard, Y.-M. Xu, L.J. Li, G.H. Cao, Z.-A. Xu, H. Ding, T. Takahashi, Proc. Natl. Acad. Sci. **106**, 7330 (2009)
19. T. Sudayama, Y. Wakisaka, T. Mizokawa, S. Ibuka, R. Morinaga, T.J. Sato, M. Arita, H. Namatame, M. Taniguchi, N.L. Saini, J. Phys. Soc. Jpn **80**, 113707 (2011)
20. P. Vilmercati, A. Fedorov, I. Vobornik, U. Manju, G. Panaccione, A. Goldoni, A.S. Sefat, M.A. McGuire, B.C. Sales, R. Jin, D. Mandrus, D.J. Singh, N. Mannella, Phys. Rev. B **79**, 220503 (2009)
21. S. Thirupathaiah, S. de Jong, R. Ovsyannikov, H.A. Dürr, A. Varykhalov, R. Follath, Y. Huang, R. Huisman, M.S. Golden, Yu-Zhong Zhang, H.O. Jeschke, R. Valentí, A. Erb, A. Gloskovskii, J. Fink, Phys. Rev. B **81**, 104512 (2010)
22. Y. Zhang, F. Chen, C. He, B. Zhou, B.P. Xie, C. Fang, W.F. Tsai, X.H. Chen, H. Hayashi, J. Jiang, H. Iwasawa, K. Shimada, H. Namatame, M. Taniguchi, J.P. Hu, D.L. Feng, Phys. Rev. B **83**, 054510 (2011)
23. Chang Liu, A.D. Palczewski, R.S. Dhaka, Takeshi Kondo, R.M. Fernandes, E.D. Mun, H. Hodovanets, A.N. Thaler, J. Schmalian, S.L. Budko, P.C. Canfield, A. Kaminski, Phys. Rev. B **84**, 020509 (2011)
24. M.L. Teague, G.K. Drayna, G.P. Lockhart, P. Cheng, B. Shen, H.-H. Wen, N.-C. Yeh, Phys. Rev. Lett. **106**, 087004 (2011)
25. F. Hardy, P. Burger, T. Wolf, R.A. Fisher, P. Schweiss, P. Adelmann, R. Heid, R. Fromknecht, R. Eder, D. Ernst, H.V. Löhneysen, C. Meingast, Europhys. Lett. **91**, 47008 (2010)
26. M. Tortello, D. Daghero, G.A. Ummarino, V.A. Stepanov, J. Jiang, J.D. Weiss, E.E. Hellstrom, R.S. Gonnelli, Phys. Rev. Lett. **105**, 237002 (2010)

27. D.N. Basov, R.D. Averitt, D. van der Marel, M. Dressel, K. Haule, Rev. Mod. Phys. **85**, 471 (2011)
28. A. Perucchi, L. Baldassarre, P. Postorino, S. Lupi, J. Phys.: Condens. Matter **21**, 323202 (2009)
29. A.A. Schafgans, S.J. Moon, B.C. Pursley, A.D. LaForge, M.M. Qazilbash, A.S. Sefat, D. Mandrus, K. Haule, G. Kotliar, D.N. Basov, Phys. Rev. Lett. **108**, 147002 (2012)
30. A. Dusza, A. Lucarelli, A. Sanna, S. Massidda, J.-H. Chu, I.R. Fisher, L. Degiorgi, New J. Phys. **14**, 023020 (2012)
31. S.J. Moon, A.A. Schafgans, S. Kasahara, T. Shibauchi, T. Terashima, Y. Matsuda, M.A. Tanatar, R. Prozorov, A. Thaler, P.C. Canfield, A.S. Sefat, D. Mandrus, D.N. Basov, Phys. Rev. Lett. **109**, 027006 (2012)
32. M. Nakajima, S. Ishida, Y. Tomioka, K. Kihou, C.H. Lee, A. Iyo, T. Ito, T. Kakeshita, H. Eisaki, S. Uchida, `arXiv:1208.1581` (2012)
33. P. Marsik, K.W. Kim, A. Dubroka, M. Rossle, V.K. Malik, L. Schulz, C.N. Wang, Ch. Niedermayer, A.J. Drew, M. Willis, T. Wolf, C. Bernhard, Phys. Rev. Lett. **105**, 057001 (2010)
34. N. Barisic, D. Wu, M. Dressel, L.J. Li, G.H. Cao, Z.A. Xu, Phys. Rev. B **82**, 054518 (2010)
35. A. Lucarelli, A. Dusza, F. Pfuner, P. Lerch, J.G. Analytis, J.-H. Chu, I.R. Fisher, L. Degiorgi, New J. Phys. **12**, 073036 (2010)
36. K.W. Kim, M. Rössle, A. Dubroka, V.K. Malik, T. Wolf, C. Bernhard, Phys. Rev. B **81**, 214508 (2010)
37. D. Wu, N. Barišić, P. Kallina, A. Faridian, A. Gorshunov, B. Drichko, L.J. Li, X. Lin, G.H. Cao, Z.A. Xu, N.L. Wang, M. Dressel, Phys. Rev. B **81**, 100512 (2010)
38. B. Gorshunov, D. Wu, A.A. Voronkov, P. Kallina, K. Ilda, S. Haindl, F. Kurth, L. Schultz, B. Holzapfel, M. Dressel, Phys. Rev. B **81**, 060509 (2010)
39. J.J. Tu, J. Li, W. Liu, A. Punnoose, Y. Gong, Y.H. Ren, L.J. Li, G.H. Cao, Z.A. Xu, C.C. Homes, Phys. Rev. B **82**, 174509 (2010)
40. R. Valdés Aguilar, L.S. Bilbro, S. Lee, C.W. Bark, J. Jiang, J.D. Weiss, E.E. Hellstrom, D.C. Larbalestier, C.B. Eom, P. Armitage, Phys. Rev. B **82**, 180514 (2010)
41. E. van Heumen, Y. Huang, D. de Jong, A.B. Kuzmenko, M.S. Golden, D. van der Marel, Eur. Phys. Lett. **90**, 37005 (2010)
42. A. Perucchi, L. Baldassarre, S. Lupi, J.Y. Jiang, J.D. Weiss, E.E. Hellstron, S. Lee, C.W. Bark, C.B. Eom, M. Putti, I. Pallecchi, C. Marini, P. Dore, Eur. Phys. J. B **77**, 25 (2010)
43. E.G. Maksimov, A.E. Karakozov, B.P. Gorshunov, A.S. Prokhorov, A.A. Voronkov, E.S. Zhukova, V.S. Nozdrin, S.S. Zhukov, D. Wu, M. Dressel, S. Haindl, K. Iida, B. Holzapfel, Phys. Rev. B **83**, 140502 (2011)
44. E.G. Maksimov, A.E. Karakozov, A.A. Voronkov, B.P. Gorshunov, S.S. Zhukov, E.S. Zhukova, V.S. Nozdrin, S. Haindl, B. Holzapfel, L. Schultz, D. Wu, M. Dressel, K. Iida, P. Kallinag, F. Kurth, J. Exp. Theor. Phys. Lett. **93**, 736 (2011)
45. T. Fischer, A.V. Pronin, J. Wosnitza, K. Ida, F. Kurth, S. Haindl, L. Schultz, B. Holzapfel, E. Schachinger, Phys. Rev. B **82**, 224507 (2010)
46. R.P.S.M. Lobo, Y.M. Dai, U. Nagel, T. Rõõm, J.P. Carbotte, T. Timusk, A. Forget, D. Colson, Phys. Rev. B **82**, 100506 (2010)
47. D. Nakamura, T. Akiike, H. Takahashi, F. Nabeshima, Y. Imai, A. Maeda, T. Katase, H. Hiramatsu, H. Hosono, S. Komiya, I. Tsukada, Physica C **471**, 634 (2011)
48. A. Yu, A. Aleshchenko, A.V. Muratov, V.M. Pudalov, E.S. Zhukova, B.P. Gorshunov, F. Kurth, K. Iida, J. Exp. Theor. Phys. Lett. **94**, 719 (2011)
49. M. Nakajima, S. Ishida, K. Kikhou, Y. Tomioka, T. Ito, Y. Yoshida, C.H. Lee, H. Kito, A. Iyo, H. Eisaki, K.M. Kojima, S. Uchida, Phys. Rev. B **81**, 104528 (2010)
50. R.E. Glover, M. Tinkham, Phys. Rev. **108**, 233 (1958)
51. D.M. Ginsberg, M. Tinkham, Phys. Rev. **118**, 990 (1960)
52. L.H. Palmer, M. Tinkham, Phys. Rev. **165**, 588 (1968)
53. S. Lee, J. Jiang, C.W. Bark, J.D. Weiss, C. Tarantini, C.T. Nelson, H.W. Jang, C.M. Folkman, S.H. Baek, A. Polyanskii, D. Abraimov, A. Yamamoto, J.W. Park, X.Q. Pan, E.E. Hellstrom, D.C. Larbalestier, C.B. Eom, Nat. Mater. **9**, 397 (2010)
54. Jiun-Haw Chu, James G. Analytis, Chris Kucharczyk, Ian R. Fisher, Phys. Rev. B **79**, 014506 (2009)
55. P. Dore, G.P. Gallerano, A. Doria, E. Giovenale, R. Trippetti, V. Boffa, Nuovo Cimento D **16**, 1803 (1994)
56. X. Xi, J. Hwang, C. Martin, D.B. Tanner, G.L. Carr, Phys. Rev. Lett. **105**, 257006 (2010)
57. S. Lupi, A. Nucara, A. Perucchi, P. Calvani, M. Ortolani, L. Quaroni, M. Kiskinova, J. Opt. Soc. Am. B **24**, 959 (2007)
58. M. Tinkham, in *Introduction to Superconductivity*, 2nd edn. (Dover Publications, 1996)
59. M. Dressel, G. Grüner, in *Electrodynamics of Solids* (Cambridge University Press, Cambridge, 2002)
60. A. Perucchi, D. Nicoletti, M. Ortolani, C. Marini, R. Sopracase, S. Lupi, U. Schade, M. Putti, I. Pallecchi, C. Tarantini, M. Ferretti, C. Ferdeghini, M. Monni, F. Bernardini, S. Massidda, P. Dore, Phys. Rev. B **81**, 092509 (2010)
61. F. Wooten, in *Optical Properties of Solids* (Academic Press, New York, 1972)
62. P. Berberich, M. Chiusuri, S. Cunsolo, P. Dore, H. Kinder, C.P. Varsamis, Infrared Phys. **34**, 269 (1993)
63. W. Zimmermann, E.H. Brandt, M. Bauer, E. Seider, L. Genzel, Physica C **183**, 99 (1991)
64. M. Ortolani, P. Dore, D. Di Castro, A. Perucchi, S. Lupi, V. Ferrando, M. Putti, I. Pallecchi, C. Ferdeghini, X.X. Xi, Phys. Rev. B **77**, 100507 (2008)
65. M. Ortolani, D. Di Castro, P. Postorino, I. Pallecchi, M. Monni, M. Putti, P. Dore, Phys. Rev. B **71**, 172508 (2005)
66. S. Lupi, L. Baldassarre, M. Ortolani, C. Mirri, U. Schade, R. Sopracase, A. Tamegai, R. Fittipaldi, A. Vecchione, P. Calvani, Phys. Rev. B **77**, 054510 (2008)
67. P. Dore, A. Paolone, R. Trippetti, J. Appl. Phys. **80**, 5270 (1996)
68. P. Dore, G. De Marzi, A. Paolone, Int. J. IR MM Waves **18**, 125 (1997)
69. M. Misra, K. Kotani, I. Kawayama, H. Murakami, M. Tonouchi, Appl. Phys. Lett. **87**, 182909 (2005)
70. A.B. Kuzmenko, Rev. Sci. Instrum. **76**, 083108 (2005)
71. L. Benfatto, E. Cappelluti, L. Ortenzi, L. Boeri, Phys. Rev. B **83**, 224514 (2011)
72. L. Baldassarre, A. Perucchi, P. Postorino, S. Lupi, C. Marini, L. Malavasi, J. Jiang, J.D. Weiss, E.E. Hellstrom, I. Pallecchi, P. Dore, Phys. Rev. B **85**, 174522 (2012)